

geometry optimization of the heat of formation of 5*H*-1-naphthalenone results in 14.8 kcal/mol for the heat of formation, or 23.1 kcal/mol above the heat of formation of the tautomeric 1-naphthol. When Woodward's rules are used, the absorption maximum of the tetraenone can be estimated to be 429 nm, or 66 kcal/mol. This compares with an absorption maximum of 293 nm (97 kcal/mol) for 1-naphthol. Assuming similar Franck-Condon factors, then $E_{0,0}$ for 1-naphthol is 31 kcal/mol greater than that for 5*H*-1-naphthalenone, and the adiabatic protonation is exothermic by 8 kcal/mol (see Figure 13). Conversely, protonation of the 2-naphtholate ion at the site of highest excited-state electron density would lead to 6*H*-2-naphthalenone (tautomeric with 8*H*-2-naphthalenone, II). Although the heat of formation of this enone using the MNDO technique is 15.4 kcal/mol, or 24.7 kcal/mol above the tautomeric 2-naphthol, the excited-state energetics for this cross-conjugated enone are much less favorable, leading to an absorption maximum of 355 nm (80 kcal/mol). Thus, this excited state is only 17 kcal/mol lower in energy than that for 2-naphthol. Adiabatic protonation becomes *endothermic* by 8 kcal/mol. The absence of proton-induced quenching in this case suggests that such quenching is possibly only when adiabatic protonation followed by rapid nonradiative decay of the tetraenone excited state is energetically feasible.

Finally, the details of the solvent/solute interactions affecting excited-state decay rates are not yet fully understood. The important aspects to be considered in investigations of these interactions are (1) the nature of the excited state, i.e., how the charge-transfer characteristics activate a group with a labile proton by removal of charge density from the heteroatom; (2) the structure of the solute/solvent complex, i.e., the ability to hydrogen bond to the solvent and thereby diabatically relax to the ground state; (3) the intrinsic structure of the solvent, i.e., the long- and short-range interactions and aggregations; and (4) the solvent

(45) MNDO calculations were performed on a VAX 780 computer using the MOPAC program. MOPAC is available from the Quantum Chemistry Program Exchange (QCPE). Dewar, M. J. S.; Thiel, W. *J. Am. Chem. Soc.* 1977, 99, 4899, 4907.

orientation; i.e., whether the proton transfer is directly possible or if solvent repositioning is necessary. New measurements in such areas as the dependence on excitation wavelength and the effect of temperature will further elaborate on the processes in the ESPT reaction of 1-naphthol.

Conclusions

The results presented here represent the first real-time measurements of the complete fluorescence kinetics of 1-naphthol in aqueous solution. Analysis of the fluorescence from the neutral species, when compared with the rise time of the fluorescence signal of the anion, shows the 1:1 coupling of the two species on the excited potential surface, indicative of an ESPT reaction. Direct observation of the weak emission from the neutral species in the steady-state emission spectra makes possible accurate analyses based on complex kinetic expressions. The combination of steady-state techniques with time-resolved methods produces the most accurate, composite picture of the kinetics of the ESPT process, especially when diabatic, proton-dependent quenching is included. Failure to include all the temporal and quantum yield measurements results in less accurate representations of the processes given by the ESPT model.^{12,15} Full kinetic analyses of 1-naphthol in H₂O and D₂O point out the importance of the solvent on the various rate processes. Comparisons of 1- and 2-naphthol present further implications regarding the effect of solute structure on the ESPT processes. The results presented here demonstrate the power of the combination of the time-resolved and steady-state methods for the study of complex systems.

Acknowledgment. This work was supported by the Office of Energy Research, Office of Basic Energy Sciences, Chemical Sciences Division of the U.S. Department of Energy under Contract DE-AC03-76SF00098. Helpful discussions with G. C. Pimentel and K. B. Eisenthal are gratefully acknowledged. The determination of the photodeuteration quantum yield by Joseph A. Schomaker of Georgia Institute of Technology is much appreciated.

Registry No. 1-Naphthol, 90-15-3.

An RRKM Approach to Vibrational Predissociation of van der Waals Clusters

D. F. Kelley*[†] and E. R. Bernstein*

Condensed Matter Sciences Laboratory, Department of Chemistry, Colorado State University, Fort Collins, Colorado 80523 (Received: April 11, 1986)

Vibrational predissociation (VP) rates are calculated for the *s*-tetrazine-Ar van der Waals complex excited to various vibronic levels of the first excited singlet state by employing RRKM theory and a serial mechanism for intramolecular vibrational redistribution (IVR) and VP. In the model presented, VP cannot take place from the optically accessed zero-order tetrazine vibronic state but follows only after IVR has populated the van der Waals modes with more energy than the cluster binding energy. The calculations can be compared with two published studies of the IVR and VP processes in the *s*-tetrazine-Ar cluster: a picosecond study of the time evolution of vibronic emission from the cluster and the free molecule following cluster excitation; and a CW emission intensity study of the cluster and free molecule following cluster excitation. Agreement between the calculation and the available experimental data is semiquantitative and as good as the agreement between the two experimental studies reported (approximately a factor of two).

Introduction

van der Waals (vdW) molecules occupy a central position in much of the theoretical and experimental study of radiationless transitions and unimolecular reaction kinetics. Since van der Waals molecules are weakly coupled systems with large intermolecular vibrational anharmonicities, large Coriolis couplings, a high density of vibrational and rotational states at low vibrational

energy, and well-defined excited "doorway" states for ready optical laser excitation, these clusters should be ideal for the investigation of vibrational predissociation. Moreover, unimolecular dissociation processes in such systems should be theoretically describable by a restricted RRKM approach.

The particular vdW molecules of concern to the work presented in this paper consist of a solute chromophore or oscillator strength bearing molecule (e.g., benzene, *s*-tetrazine, etc.) associated with a solvent molecule (e.g., argon, methane, etc.). Only the chro-

* Alfred P. Sloan Fellow.

mophore in this cluster has optically accessible states. Typically, the solvent molecule does not have molecular vibrations which need to be considered in the vibrational dynamics of the clusters. Such van der Waals clusters are most easily produced in a supersonic molecular jet expansion which generates cold isolated clusters.

In this work we address two vibrational processes that can occur in vdW molecules: intramolecular vibrational redistribution (IVR) of vibrational energy and vibrational predissociation (VP) of the vdW cluster. IVR in a rotationally and vibrationally cold cluster undergoing no collisions is the dephasing or time evolution of the optically prepared or "doorway" state. The state accessed by laser excitation (i.e., the state carrying all the oscillator strength) is that coherent superposition of cluster eigenstates for which all the excitation is in the chromophore zero-order vibronic state and the vdW modes are not excited. This linear combination of cluster eigenstates subsequently dephases into different zeroth order chromophore and vdW vibrations which have the same total energy. Thus, during the IVR process, lower energy chromophore vibrational states and the vdW modes required for energy conservations become populated. The IVR process is typically modeled and studied in an excited electronic state of the chromophore. VP involves the dissociation of the cluster into chromophore and solvent molecules: the chromophore typically retains the electronic excitation and perhaps some or all of the excess vibrational energy not required for bond rupture.

If a cluster is optically excited to a vibronic state carrying enough excess vibrational energy to rupture the vdW bond, both IVR and VP processes can take place. If the excess vibrational energy is below the cluster binding energy, then only IVR can redistribute the excess vibrational energy in the accessed vibronic state. Of course, in general IVR and VP must compete with radiative processes, intersystem crossing, and internal conversion.

Existing theory of VP suggests that IVR and VP are simultaneously occurring "parallel processes" if the optically accessed "doorway" state has more excess vibrational energy than the cluster binding energy.¹ In this approach VP can occur directly from the optically accessed zero-order chromophore or doorway state. Most authors²⁻⁴ discussing VP and CW laser experimental results for IVR/VP take this point of view either explicitly or implicitly: both Levy³ and Rice⁴ take this approach in analyzing their data for the tetrazine- and benzene-argon clusters. Levy et al.³ interpret CW laser-excited dispersed emission data using the parallel mechanism and report separate IVR and VP rate constants for tetrazine-argon. Rice et al.⁴ are correctly careful, however, not to distinguish between IVR and VP rates based on CW laser measurements of dispersed emission alone. These authors call the apparent relaxation processes simply IVR/VP. Nonetheless, both groups report branching ratios, discuss propensity rules for various IVR and VP channels, and present modes with "special" relationships to the VP mechanism.

In this paper we report calculations embracing a more standard approach to VP based on RRKM theory of unimolecular reactions and on the assumption that VP *does not* take place from the optically accessed doorway state. This model can be called a serial or sequential mechanism for IVR and VP; IVR must occur before VP in this approach. The initial excess vibrational energy in the vibronic excitation is first distributed between the vdW and chromophore modes. This step can be the slow, rate-controlling step in the vibrational dynamics, or it can be comparatively fast. These rates will actually depend in some measure on the density of vdW states at the energy of the vdW mode excitation in the final state. As the energy appears in the vdW modes, then VP can occur based on a restricted (to vdW vibrational phase space) RRKM mechanism. The role of the chromophore vibrational

mode initially accessed in the cluster and the importance of the remaining free chromophore vibrational excitation following VP are greatly reduced in the serial mechanism.

The mode accessed by laser optical excitation is important only in that the linear combination of cluster eigenstates is predetermined: dephasing or IVR processes then take place as prescribed by the cluster Hamiltonian. VP in this serial RRKM mechanism then depends only on the total energy in the vdW modes and the (assumed rapid) vdW mode to vdW mode IVR.

This paper reports calculations based on the above serial approach to IVR and VP, employing RRKM theory to arrive at unimolecular rate constants for VP. In particular, we employ cluster parameters appropriate for tetrazine-argon clusters and are able to reproduce propensity rules, special modes for VP, etc. based only on competing sequential IVR and VP pathways. The calculations assume a single chromophore to vdW mode IVR rate, a vdW mode density of states factor for the appropriate vdW mode energy, fast vdW mode to vdW mode IVR, and (restricted) RRKM theory for VP.

Theory and Computational Techniques

The calculations reported here assume sequential IVR/VP pathways. Several assumptions are implicit in this approach. Since vdW modes are strongly coupled to each other by anharmonic and Coriolis interactions and their frequencies are so different from those of the chromophore modes, we assume that chromophore to van der Waals mode IVR occurs slowly compared to IVR between the van der Waals modes. Rapid IVR among the vdW modes results in the applicability of a "restricted" RRKM theory to describe the VP process. This approach differs from conventional RRKM theory in that only the vdW modes are considered to take part in the VP process. This means that the calculated VP rate will depend only upon the amount of vibrational energy in the vdW modes.⁵

Immediately following photoexcitation, all of the vibrational energy will be in the optically accessed chromophore vibration, and the VP rate will be zero. As chromophore to vdW mode IVR proceeds, larger amounts of energy will be found in the vdW modes. The VP rate will become nonzero when the vdW mode energy exceeds the dissociation energy and will continue to increase with increasing vdW mode energy. The RRKM dissociation rate is approximately given by

$$k_a(E_{vdw}) = \frac{1}{h} \frac{\sum P_v(E_{vdw}^+)}{N(E_{vdw})}$$

in which E_{vdw}^+ is the amount of excess vdW mode energy above the dissociation threshold, $E_{vdw}^+ = E_{vdw} - E_0$ (E_0 is the dissociation energy), $\sum P_v(E_{vdw}^+)$ is the sum of vibrational states excluding those associated with the reaction coordinate, and $N(E_{vdw})$ is the density of vibrational states.

The sums and densities of states may be easily evaluated with an extended Beyer-Swinehart direct count algorithm.⁶ The van der Waals frequencies (10, 12, and 43 cm^{-1}) and anharmonicities (0.03, 0.03, and 1.15 cm^{-1}) are calculated with a atom-atom potential model.⁷ The dissociation energy is taken to be 350 cm^{-1} . The stretch mode is taken to be the reaction coordinate.

The calculations reported here are made under the assumption that the rate of IVR between any two chromophore vibrational states depends only upon the total number of quanta (chromophore plus vdW modes) exchanged during the transition. This treatment is justified by the argument that multiquanta transitions will have small Franck-Condon factors and therefore be less probable than transitions involving fewer quanta. This simple treatment also excludes the possibility of favored relaxation pathways and IVR propensity rules. Specifically, the probability of a transition between chromophore levels j and i in a short time interval, Δt , is given by

(1) Beswick, J. A.; Jortner, J. *Chem. Phys. Lett.* **1977**, *49*, 13. *J. Chem. Phys.* **1978**, *68*, 2277. Beswick, J. A.; Delgado-Barrow, G.; Jortner, J. *Ibid.* **1979**, *70*, 3895.

(2) Bernstein, E. R.; Law, K.; Schauer, M. *J. Chem. Phys.* **1984**, *80*, 207.

(3) Brumbaugh, D. V.; Kenney, J. E.; Levy, D. H. *J. Chem. Phys.* **1983**, *78*, 3415.

(4) Stephenson, T. A.; Rich, S. A. *J. Chem. Phys.* **1984**, *81*, 1083.

(5) For a good discussion of RRKM theory see Robinson, P. J., Holbrook, K. A. *Unimolecular Reactions*; Wiley: New York, 1972.

(6) Stein, S. E.; Rabinovitch, B. S. *J. Chem. Phys.* **1973**, *58*, 2438.

(7) Menapace, J. A.; Bernstein, E. R. submitted to *J. Chem. Phys.*

$$P_{ij} = A \exp(-\Delta v) \exp(-(E_j - E_i)/h\nu_{\max}) \rho(E_{\text{ex}} - E_i) \Delta t \quad i \neq j \quad (1)$$

in which Δv is the total number of chromophore quanta exchanged, ν_{\max} is the highest vdW mode frequency, E_{ex} is the excitation energy, and $\rho(E_{\text{ex}} - E_i)$ is the density of vdW "receiving" vibrational states at an energy of $(E_{\text{ex}} - E_i)$. $\rho(E_{\text{ex}} - E_i)$ will be discussed in more detail later. A $6a^2$ to $16a16b$ transition has $\Delta v = 4$, loss of two quanta in the $6a$ mode, and an increase of one quanta in both the $16a$ and $16b$ modes; similarly, a $6a^2$ to $6a$ transition has $\Delta v = 1$. A is the only adjustable parameter in the model and scales the off-diagonal ($i \neq j$) transition probabilities.

Transition probabilities involving large changes of chromophore and vdW energy are dominated by the second exponential term in eq 1. This term results in an exponential "energy gap law" when a large number of quanta are transferred into the vdW modes.

The density of vdW receiving states, $\rho(E_{\text{vdW}})$ ($E_{\text{vdW}} = E_{\text{ex}} - E_i$), is difficult to evaluate accurately. At low energies ($\leq 250 \text{ cm}^{-1}$), $\rho(E_{\text{vdW}})$ is equal to 1.0 at specific energies corresponding to overtones and combinations of the vdW modes and zero at all other energies. IVR from the initially excited level to a lower chromophore level requires that a specific amount of energy be lost from the chromophore modes and deposited into the vdW modes. A transition can occur only if a vdW combination or overtone mode exists at the exact energy corresponding to the energy difference between chromophore energies. The excited chromophore Q branches have widths of only about 0.1 cm^{-1} (for tetrazine-Ar) and a very close energy match ($\sim 0.1 \text{ cm}^{-1}$) between vdW and chromophore modes is therefore required.⁸ Whether or not vdW modes can acquire the exact energy in question is determined by the exact values of the frequencies, anharmonicities, etc. of each vdW mode; these exact coincidences are, therefore, extremely difficult to predict. On the other hand, at large energies the density of vdW states becomes quite large. When the density of states is much greater than 10 states/ cm^{-1} , the probability of having a receiving state at the proper energy is quite high. This occurs at about $250\text{--}300 \text{ cm}^{-1}$ of vdW energy for the tetrazine-Ar system. At very low energies ($< 100 \text{ cm}^{-1}$) the probability of an energy match is quite low. We emphasize that in the intermediate energy ($100\text{--}300 \text{ cm}^{-1}$) region we cannot determine if a receiving vdW vibrational state will exist at any particular energy.

At the highest energies, several vdW modes may be within $\sim 0.1 \text{ cm}^{-1}$ of a specific energy, and therefore several receiving states will be available at a given chromophore energy.

Two simple approximate forms can be chosen to model the vdW density of states $\rho(E_{\text{vdW}})$: 1. $\rho(E_{\text{vdW}}) = 1$ in all but the very lowest energies ($< 50\text{--}100 \text{ cm}^{-1}$). 2. $\rho(E_{\text{vdW}})$ is given by a smoothed function of the total density of vdW states. Both assumptions permit population of almost all of the chromophore complex vibrational levels even at energies less than 200 cm^{-1} . The latter assumption is made in the calculation reported here.

With the above assumptions and approximations, eq 1 permits the calculation of the off-diagonal elements of the entire transition probability matrix. The diagonal elements are then calculated to conserve total probability, i.e.

$$1 = \sum_i P_{ij} \quad \text{for all } j$$

Thus, one adjustable parameter is used to describe the entire IVR process, and the same parameter is used to describe IVR for all levels of initial excitation.

The transition probability matrix can then be used along with the calculated RRKM VP rates and known tetrazine photochemical fragmentation rates to calculate the time-dependent populations of each complexed and uncomplexed chromophore vibrational level. From these populations, total (time integrated) dispersed emission spectra can also be calculated. The iterative algorithm of this calculation is outlined below.

Two vectors are defined such that each element represents the population in a specific chromophore vibrational state. One vector

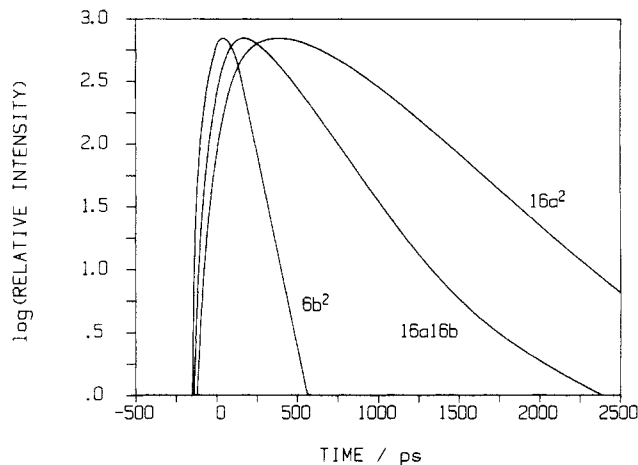


Figure 1. Buildup and decay curves for tetrazine-Ar emission from vibronic states $6b^2$, $16a^2$, and $16a^116b^1$ following excitation of the $6b^2$ levels of the cluster. The calculated curves are convolved with a 150-ps fwhm triangular instrument response function to facilitate comparison with the experimental results of ref 9. The $16a^2$ kinetic curve is used to fix the transition probability matrix parameter A as discussed in the text (see eq 1).

represents the complex while the other represents the uncomplexed molecule.

Initially, we have

$$N_c(t=0) = \begin{bmatrix} 1 \\ 0 \\ 0 \\ \vdots \\ 0 \\ 0 \end{bmatrix} \quad N_{nc}(t=0) = \begin{bmatrix} 0 \\ 0 \\ \vdots \\ 0 \\ 0 \end{bmatrix}$$

complexed uncomplexed

in which unit population has been put into a specific vibrational level of the complexed molecule. As discussed above, IVR over a specific time interval is simulated by multiplication of this vector by the transition probability matrix. Similarly, fragmentation and vibrational predissociation may be simulated by matrix multiplications.

We define a VP matrix D such that $D_{ij} = (1 - k_i \Delta t) \delta_{ij}$ with k_i the RRKM VP rate at energy $E_{\text{vdW}} = E_{\text{ex}} - E_i$, and a tetrazine photochemical fragmentation rate matrix F such that $F_{ij} = (1 - k'_i \Delta t) \delta_{ij}$ with k'_i the fragmentation rate of level i . k'_i values are given in ref 3. Temporal evolution of the population vectors are then given by

$$N_c(t+\Delta t) = F D N_c(t)$$

$$N_{nc}(t+\Delta t) = F N_{nc}(t) + (1 - D) N_c(t)$$

In all cases the time interval is chosen to be sufficiently small that further reduction has no effect on the calculated results.

Results and Discussion

The time-dependent populations of each complexed and uncomplexed chromophore vibrational level are calculated following excitation of the $6b^2$, $6a^1$, and $16a^2$ levels of the tetrazine-Ar cluster. Figure 1 shows the normalized populations of the $6b^2$, $16a^116b^1$, and $16a^2$ complex levels following $6b^2$ excitation. The one adjustable parameter of the model (discussed above) has been set to give good agreement with the $16a^2$ level time-resolved results reported by Rettschnick et al.⁹ These time-resolved studies⁹ report a 325-ps lifetime of the $16a^2$ level. In all calculations the constant A of eq 1 has been set to a value of 0.022, which reproduces this lifetime exactly. Comparison of Figure 1 with Figure 2 of ref 9

(8) Brumbaugh, D. V.; Haynan, C. A.; Levy, D. H. *J. Mol. Spectrosc.* **1982**, *94*, 316.

(9) Heppener, M.; Kunst, A. G. M.; Bebelaar, D.; Rettschnick, R. P. H. *J. Chem. Phys.* **1985**, *83*, 5341.

shows that the agreement of the calculated and experimentally determined $16a^2$ populations is nearly quantitative over the entire time range reported.

These figures also show reasonably good agreement between calculations and experiments for the $16a^116b^1$ and $6b^2$ complex populations. The calculated $16a^116b^1$ decay is somewhat faster than the experimentally determined rate. Thus, once the adjustable parameter in the theory has been set for one complex decay curve, the other decay curves are fit nearly quantitatively without further adjustment.

The applicability of the presented model can be further tested by comparison to the steady-state spectra reported by Levy et al.³ These studies have determined the total (time-integrated) emission from each complexed and uncomplexed chromophore level following single vibronic level excitation. Weighting emission intensities by the appropriate reciprocal Franck–Condon factors yields the time-integrated populations. These quantities can also be calculated by integrating the calculated time-dependent populations. In all cases the one adjustable parameter of the model was maintained at the value required to fit the $16a^2$ decay reported in Rettschnick's time-resolved experiments.

One caveat regarding these calculations needs to be emphasized: IVR from the initially excited complex level to lower complex levels requires that the density of vdW states be nonzero at an energy corresponding to the energy difference of the chromophore levels. At low vdW energies ($<250\text{ cm}^{-1}$) this condition may not be met for some sets of chromophore levels. As a result, some chromophore levels may be "avoided" by the IVR process simply due to energy conservation restrictions. Due to the large density of vdW states at higher energies this is likely to occur only for levels which are within about 250 cm^{-1} of the initially excited level. The calculations reported here have taken the density of vdW states to be a smooth, continuous function that is nonzero even at low energies. This permits population to relax through all of the vibrational levels. The calculated populations are therefore unreliable for the levels immediately below the initially excited level.

The calculated (time-integrated) populations and the populations determined from Levy's results following $6b^26a^1$ and $16a^2$ excitation are given in Table I. (Levy³ has also reported spectra following excitation of the higher lying $16a^216a^1$ and $6a^2$ modes. Due to the large number of levels involved, no attempt to analyze these results has been made.)

As stated above, we have selected the one adjustable parameter of the model to fit the time-resolved $16a^2$ data following $6b^2$ excitation. One must therefore examine the level of consistency between Rettschnick's time-resolved and Levy's steady-state data. Such a comparison is possible only for the $16a^116b^1$ and $16a^2$ levels following $6b^2$ excitation. Time-integrated (static) emission intensities can be calculated from the experimental time-resolved results. The total emission intensity of the i th level is given by

$$I_j = N_j f_j \frac{k_{\text{rad}}}{k_{\text{tot}}}$$

in which N_j is the total number of molecules that enter state j , f_j is the Franck–Condon factor of the emission line being observed, and k_{rad} and k_{tot} are the radiative and total decay rates, respectively.

The ratio of $16a^116b^1$ to $16a^2$ emission intensities may be calculated from the following considerations. The Franck–Condon factor for the $16a^116b^1$ sequence band is 0.96, and the measured decay time (k_{tot}) is about 470 ps. The $16a^2$ Franck–Condon factor is also 0.96 and the total lifetime is 325 ps. However, the $16a^116b^1$ state has a fragmentation lifetime of ~ 1.45 ns. These lifetimes indicate that not more than $\sim 67\%$ of tetrazine–Ar clusters in the $16a^116b^1$ state decay via IVR to the $16a^2$ level. (The fraction would be less if VP could occur from the $16a^116b^1$ level or if IVR could occur to levels other than the $16a^2$ level.) Furthermore, the slow risetime of the $16a^2$ emission reported in ref 9 precludes the possibility of this state being populated directly from the initially excited $6b^2$ level. The total number of molecules which enters the $16a^2$ level is, therefore, not more than $\sim 67\%$ of the number that enters the $16a^116b^1$ state.

TABLE I: Relative Time-Integrated Populations of Complex Bare Chromophore Vibronic Levels^a

mode	tetrazine–Ar complex		uncomplexed tetrazine	
	exptl ^c	calcd ^b	exptl ^c	calcd
6b ² Excitation				
6b ²	1.0	1.0	0	0
16a ³	0	(0.025)	0	0
6a	0	(0.026)	0	0
17b	0	(0.045)	0	0
16a16b	0.069	(0.016)	0	0
16a6b	0	(0.008)	0	0
4	0	(0.020)	0	0
16a ²	0.061	0.032	0	0
16b	0	~0	0.068	0.021
6b	0	~0	0	~0
16a	0	~0	0.196	0.044
0	0	~0	0	~0
6a Excitation				
6a	1.0	1.0	0	0
17b	0	(0.0)	0	0
16a16b	0	(0.14)	0	0
16a6b	0	(0.07)	0	0
4	0	(0.13)	0	0
16a ²	0.07	0.094	0	0
16b	0.005	0.011	0	0
6b	0.0	0.0	0	0
16a	0.0	0.0	0.19	0.14
0	0.0	0.0	0	0
16a Excitation				
16a ²	1.0	1.0	0	0
16b	0	(0.03)	0	0
6b	0	(0)	0	0
16a	0.15	0.14	0	0
0	0	0	0.096	0.07

^aNote that, as discussed in the text, the agreement between the experimental data quoted here (ref 3) and that quoted in Figure 1 (ref 9) is not better than a factor of two. The constants employed fit the data of ref 3 are obtained from the time-resolved data of ref 9. The point is fully discussed in the text. ^bValues in parentheses are unreliable due to the low density of states. See text. ^cTaken from the results reported in ref 3.

A lower limit to the ratio of $16a^116b^1$ to $16a^2$ emission intensities can now be calculated. This ratio calculated from the time-resolved results is ≥ 2.2 . The same ratio, determined from the static spectroscopic results, is ~ 1.1 . This analysis demonstrates that the two sets of results are quantitatively inconsistent by about a factor of 2. Since the calculations are constrained to fit the $16a^2$ experimental time-resolved data, no better than a factor two agreement between the calculated results and the static spectroscopic results can reasonably be expected. In most cases the agreement is within a factor of about three. In kinetic calculations, agreement to within a factor of three is usually considered acceptable. The calculated relaxed emission intensities are, in most cases, somewhat below the values determined from the static spectra. We believe that this is due to the approximations made in $\rho(E_{\text{vdW}})$. For example, if $\rho(E_{\text{vdW}})$ is taken to be constant (i.e., the number of receiving states is always one) then the calculated relaxed emission intensities are generally somewhat larger than the observed values; however, this approximation yields less satisfactory agreement with the time resolved results.

Most importantly, over the energy ranges of applicability, these calculations accurately reproduce the "propensity rules" seen in Levy's data. Specifically, following $6b^2$ excitation our calculations predict little or no emission from the 0^0 , $16a^1$, $6b^1$, and $16b^1$ levels of the complex and little or no emission from the 0^0 and $6b^1$ levels of the uncomplexed tetrazine. The calculations predict emission only from the $16a^1$ and $16b^1$ levels of the uncomplexed tetrazine. Table I shows that all of these predictions are borne out by the experimental results.

Calculations predict little or no emission from the $6b^1$, $16a^1$, and 0^0 levels of the complex and little or no emission from the

0^0 level of the uncomplexed tetrazine following $6a^1$ excitation of the complex. The calculations also predict very little 0^0 complex emission following $16a^1$ excitation of the complex. In all cases these predictions and the experimentally observed results are in complete agreement.

Conclusions

This simple, one-parameter RRKM model is in semiquantitative agreement with all the static and time-resolved data for which

comparison is possible. The detailed validity of this model can be unambiguously tested only by direct time-resolved spectroscopic studies of both complexed and uncomplexed molecules in specific vibrational states.

Acknowledgment. This work was supported by the National Science Foundation.

Registry No. Ar, 7440-37-1; s-tetrazine, 290-96-0.

State-Selective Photochemistry of Singlet Oxygen Precursors: Kinetics and Wavelength Dependence of the Photodissociation of Anthracene Endoperoxides

K. B. Eisenthal,* N. J. Turro,* C. G. Dupuy,[†] D. A. Hrovat,[‡] J. Langan, T. A. Jenny,[§] and E. V. Sitzmann

Department of Chemistry, Columbia University, New York, New York 10027 (Received: April 15, 1986)

The photochemical behavior of the two isomeric endoperoxides (9,10-PMO₂ and 1,4-PMO₂) of 1,4-dimethyl-9,10-diphenylanthracene was found to differ in their kinetics and reaction efficiencies. Consistent with the work of Rigaudy et al. and Brauer et al. on a related endoperoxide we find that the generation of ¹O₂ is wavelength dependent, occurring from upper excited singlet states of the endoperoxide, whereas bond cleavage of the O-O endoperoxide bond occurs principally from the lowest excited singlet and triplet states. Results of picosecond kinetics and absolute quantum yield measurements are discussed in terms of various concerted and nonconcerted mechanisms for the formation of ¹O₂ and the anthracene fragment.

Introduction

Whether it is a state-dependent reaction of an intermediate or of an excited-state precursor, the observation of state-selective chemistry is important in the determination of reaction mechanisms. The case of wavelength-dependent photochemistry is particularly interesting since the initially prepared excited state places stringent constraints on the chemical decay pathway. As a general rule, organic photoreactions in solution do not occur efficiently from upper electronically excited states (S_n or T_n , where $n \geq 2$) due to the very rapid relaxation to the lowest excited state of the same symmetry (Kasha's rule).¹ The photochemical reactions of the 9,10- and the 1,4-endoperoxides^{3,4} of anthracene are conspicuous exceptions to this general rule. For example, Rigaudy³ first reported the wavelength dependence of product formation in the photochemistry of anthracene endoperoxides, and later Brauer et al.⁴ convincingly demonstrated that the wavelength dependence results from a higher reactivity of upper singlet states (S_n , $n \geq 2$) toward fragmentation into the parent anthracene and molecular oxygen. Brauer et al.⁴ also found that molecular oxygen was produced in its excited singlet state, thus demonstrating that the upper state reaction occurs adiabatically. Picosecond work on a 1,4-endoperoxide anthracene derivative also showed the adiabaticity of photofragmentation for upper excited singlet states by finding that the anthracene fragment was formed in its excited singlet state although through a minor dissociative route.¹² In addition to being of intrinsic interest because of its special status as an upper state, adiabatic process, the photochemistry of anthracene endoperoxides has attracted attention because of the possibility of correlating experiments with the theoretical calculations of Kearns and Khan,⁵ who predicted the state-selective (S_1 , O-O bond cleavage; S_2 , concerted adiabatic cleavage of the C-O bonds) photochemistry of aromatic endoperoxides. Furthermore, the thermolyses of anthracene endoperoxides are exceptional in that singlet molecular oxygen, a species of wide

chemical importance in its own right,⁶ is produced in a chemiluminescent process.⁷ Thus, since the anthracene endoperoxides possess unusual and intriguing ground- and excited-state behavior, it is of value to investigate and compare systematically the thermal chemistry and photochemistry for a selected set of structures. We report here an investigation of the chemical and physical properties of the excited electronic states of two isomeric endoperoxides of 1,4-dimethyl-9,10-diphenylanthracene: 9,10-PMO₂ and 1,4-PMO₂ (Scheme I), two substances whose thermal chemistry and thermochemical parameters have been established.^{7a} The salient results of our photochemical studies are (1) the observation of different wavelength dependences of the photochemistry of 9,10-PMO₂ and 1,4-PMO₂, which is accounted for by the different reactivities of upper excited singlet π, π^* states (S_n , $n \geq 2$), (2) direct spectroscopic determination of the singlet molecular oxygen produced from the photolysis of 9,10-PMO₂ and 1,4-PMO₂ as well as direct spectroscopic measurement of the dynamics of formation of the parent anthracene (PM) from the photoexcited endoperoxide, and (3) spectroscopic kinetic evidence consistent with a

(1) Turro, N. J.; Ramamurthy, V.; Cherry, W.; Farneth, W. *Chem. Rev.* **1978**, *78*, 125.

(2) (a) Forster, Th. *Pure Appl. Chem.* **1973**, *34*, 225. (b) Turro, N. J.; McVey, J.; Ramamurthy, V.; Lechtken, P. *Angew. Chem.* **1979**, *91*, 597.

(3) Rigaudy, J.; Breliere, C.; Schribe, P. *Tetrahedron Lett.* **1978**, 687.

(4) (a) Drews, W.; Schmidt, R.; Brauer, H. D. *Chem. Phys. Lett.* **1980**, *70*, 84. (b) Schmidt, R.; Drews, W.; Brauer, H. D. *J. Photochem.* **1982**, *18*, 365. (c) Schmidt, R. *Ibid.* **1983**, *23*, 379. (d) Brauer, H. D.; Schmidt, R. *Ibid.* **1984**, *27*, 17. (e) Gabriel, R.; Schmidt, R.; Brauer, H. D. *Z. Phys. Chem. Neue Folge* **1984**, *141*, 41. (f) Schmidt, R.; Schaffner, K.; Trost, W.; Brauer, H. D. *J. Phys. Chem.* **1984**, *88*, 956.

(5) (a) Kearns, D. R.; Khan, A. U. *Photochem. Photobiol.* **1969**, *10*, 193. (b) Kearns, D. R. *Chem. Rev.* **1971**, *71*, 395. (c) Kearns, D. R. *J. Am. Chem. Soc.* **1969**, *91*, 6554.

(6) Wasserman, H. H.; Murray, R. W. *Singlet Oxygen Academic*: New York, 1979.

(7) (a) Turro, N. J.; Chow, M. F.; Rigaudy, J. *J. Am. Chem. Soc.* **1981**, *103*, 7218. (b) Wasserman, H. H.; Scheffer, J. R.; Cooper, J. L. *Ibid.* **1972**, *94*, 4991.

(8) For details of the product analysis, see: Hrovat, D. A., Ph.D. Dissertation, Columbia University, New York, NY, 1984.

(9) (a) Ting, C. H. *Chem. Phys. Lett.* **1965**, *1*, 335. (b) Meyer, Y. H.; Astier, R.; Leclercq, J. M. *J. Chem. Phys.* **1972**, *56*, 801.

(10) Kobayashi, T.; Nagakura, S. *Chem. Phys. Lett.* **1976**, *43*, 49.

(11) Jenny, T. A.; Turro, N. J. *Tetrahedron Lett.* **1982**, *23*, 2923.

* Present address: IBM Research Center, Yorktown Heights, NY 10598.

[†] Present address: Department of Chemistry, University of Washington, Seattle, WA 98105.

[‡] Present address: Institut de Chimie Organique, Universite de Fribourg, Switzerland.